



Published in final edited form as:

J Chem Inf Model. 2007 ; 47(6): 2416–2428. doi:10.1021/ci700271z.

Search for Non-nucleoside Inhibitors of HIV-1 Reverse Transcriptase using Chemical Similarity, Molecular Docking, and MM-GB/SA Scoring

Gabriela Barreiro, Cristiano R. W. Guimarães, Ivan Tubert-Brohman, Theresa M. Lyons, Julian Tirado-Rives, and William L. Jorgensen*

Department of Chemistry, Yale University, 225 Prospect Street, New Haven, Connecticut 06520-8107

Abstract

A virtual screening protocol has been applied to seek non-nucleoside inhibitors of HIV-1 reverse transcriptase (NNRTIs) and its K103N mutant. First, a chemical similarity search on the Maybridge library was performed using known NNRTIs as reference structures. The top-ranked molecules obtained from this procedure plus 26 known NNRTIs were then docked into the binding sites of the wild-type reverse transcriptase (HIV-RT) and its K103N variant (K103N-RT) using Glide 3.5. The top-ranked 100 compounds from the docking for both proteins were post-scored with a procedure using molecular mechanics and continuum solvation (MM-GB/SA). The validity of the virtual screening protocol was supported by (i) testing of the MM-GB/SA procedure, (ii) agreement between predicted and crystallographic binding poses, (iii) recovery of known potent NNRTIs at the top of both rankings, and (iv) identification of top-scoring library compounds that are close in structure to recently reported NNRTI HTS-hits. However, purchase and assaying of selected top-scoring compounds from the library failed to yield active anti-HIV agents. Nevertheless, the highest-ranked database compound, S10087, was pursued as containing a potentially viable core. Subsequent synthesis and assaying of S10087 analogs proposed by further computational analysis yielded anti-HIV agents with EC₅₀ values as low as 310 nM. Thus, with the aid of computational tools, it was possible to evolve a false positive into a true active.

Introduction

HIV/AIDS has caused more than 20 million deaths since 1981, and an estimated 40 million people are currently HIV-positive.¹ Despite the availability of the highly active antiretroviral therapy (HAART), 3 million HIV/AIDS-related deaths occurred in 2006. HAART suppresses HIV replication through administration of a combination of nucleotide (NtRTIs), nucleoside (NRTIs), and non-nucleoside reverse transcriptase inhibitors (NNRTIs), and HIV protease inhibitors.¹ The target for the first three drug classes is HIV-1 reverse transcriptase (HIV-RT), which is vital to replication of the HIV-1 virus by converting its single-stranded RNA into a double-stranded DNA.²⁻⁴ HIV-RT is a 1000-residue heterodimer consisting of 66-kDa (p66) and 51-kDa (p51) subunits.^{5,6} The present study focuses on NNRTIs, which bind to an allosteric site that is ca. 15– \AA from the polymerase active site in the p66 subunit, and thus provide noncompetitive inhibition. Many crystal structures of HIV-RT complexed with NNRTIs have been reported.⁷⁻¹⁹ To date, three NNRTIs have been approved for clinical use: nevirapine (Viramune®), delavirdine (Rescriptor®), and efavirenz (Sustiva®).²⁰ Other

*Corresponding author e-mail: william.jorgensen@yale.edu.

promising NNRTIs that have been developed include HEPT derivatives,²¹ TIBO derivatives (i.e., 8-Cl-TIBO (tivicirapine)),²²⁻²³ pyridinone derivatives (L-697,661),²⁴ loviride (alpha-APA),²⁵ the imidazole derivative S-1153 (capravirine),²⁶ PTT derivatives,^{27,28} MKC-442 (emivirine),²⁹ DPC082 and DPC083,³⁰ QXPT derivatives,³¹ DABO derivatives,³² thiocarboxanilides (UC-781),³³ and DAPY derivatives (TMC-125).^{34,35}

A major limitation to the success of therapy with NNRTIs is the rapid development of drug-resistant mutants. One of the most common resistances that emerge during failure of an NNRTI-containing regimen is a lysine to asparagine mutation at codon 103 (K103N). This mutation confers cross-resistance to all currently available NNRTIs.³⁶⁻³⁷ The activities of all three FDA-approved NNRTIs mentioned above are diminished by factors of 40–200 due to the K103N mutation.³⁸

A major focus of the drug discovery efforts to obtain new NNRTIs is to identify compounds that have activity against both the wild-type and mutants. One way to search for new compounds is to screen databases of molecular structures. As an initial step, it is possible to retrieve potentially active molecules from these databases applying a *chemical similarity search*.³⁹ This type of search is based on the *Similar Property Principle*,⁴⁰ which states that structurally similar molecules should reveal similar physicochemical and biological properties.⁴¹ This approach involves the specification of one or more molecules in the database, the *target structures*, characterized by one or more descriptors. This set is compared with the corresponding sets of descriptors for each of the molecules in the database. These comparisons enable the calculation of a measure of similarity between the target structures and each of the database structures. As a second step, assuming a high-resolution crystal structure of the protein is available, the best-ranked molecules identified by the chemical similarity search can be docked into the binding site to narrow down the number of potentially active molecules.⁴²

The goal of this study is to seek new non-nucleoside inhibitors of HIV-RT and its K103N mutant. The top-ranked molecules from a similarity search on the Maybridge database were selected and docked into the binding sites of HIV-RT and its K103N variant (K103N-RT). Nine previously reported inhibitors designed by our group⁴³ and known HIV-RT inhibitors were also docked. To circumvent limitations of the docking scoring function, particularly those associated with estimation of dehydration and intramolecular strain for the ligands upon binding, the top-scoring molecules obtained from docking were post-scored with a molecular mechanics and continuum solvation model, as described below.

Theoretical Methods

Database Searching

The intermolecular structural similarity can be measured through distance and association coefficients. Distance coefficients quantify the degree of difference between two molecules and have been extensively used when real-valued variables (physicochemical or biological descriptors) are employed; the Euclidean distance is an example (eq 1), where $D_{A,B}$ is the distance or degree of similarity between molecules A and B, x_{jA} and x_{jB} are the property values for A and B, and w_j is the corresponding descriptor weight.

$$D_{A,B} = \left[\sum_{j=1}^n w_j (x_{jA} - x_{jB})^2 \right]^{1/2} \quad (1)$$

Association coefficients are used with real-value descriptors or binary data, and are often normalized to lie within the range of zero (no similarity at all) and unity (identical sets of descriptors); the Tanimoto coefficient is an example (eq 2), where $S_{A,B}$ is the degree of similarity between molecules A and B, and x_{jA} and x_{jB} are the property values for A and B.

$$S_{A,B} = \frac{\sum_{j=1}^n x_{jA} x_{jB}}{\sum_{j=1}^n x_{jA}^2 + \sum_{j=1}^n x_{jB}^2 - \sum_{j=1}^n x_{jA} x_{jB}} \quad (2)$$

Initially, all molecules from the Maybridge database (ca. 70,000 molecules) were processed by QikProp 2.3, which computed 36 properties for each compound. These properties were used to run the chemical similarity searches, carried out by QikSim 2.3.⁴⁴ The program computed the Euclidean and Tanimoto coefficients for all compounds with respect to the average of physicochemical and biological properties of 26 known NNRTIs (Figure 1). It was previously demonstrated that the property space for NNRTIs only overlaps a small subspace of the property space for the Maybridge library.⁴⁵ In addition, enrichment factors were calculated and included running tallies of the number of known NNRTIs that were found in proceeding from the best ranked molecules to the worst. To maximize the retrieval of known NNRTIs among the first 5% of the best ranked molecules, a genetic algorithm was employed to guide the selection of descriptors for the calculation of both Euclidean and Tanimoto coefficients and to optimize the descriptor weights for the former. Specifically, the genetic algorithm was used to obtain the set of descriptors and weights that maximize the Tanimoto and Euclidean enrichment factors simultaneously. The top-ranked compounds obtained by this procedure were then used in the molecular docking calculations.

Docking

The crystal structures for HIV-RT complexed with the inhibitor UC-781 (PDB ID: 1rt4) and the K103N variant complexed with the inhibitor TMC-125 (PDB ID: 1sv5) were employed in the docking calculations performed with Glide 3.5.^{46a,b} The complexes were submitted to a series of restrained, partial minimizations using the OPLS-AA force field.⁴⁷ All compounds used in the docking calculations were submitted to a pre-minimization with the MMFF94 force field⁴⁸ using a “4r” distance-dependent dielectric constant. In order to accommodate the fact that the protein structure used for docking is not in general optimal for a particular ligand, the van der Waals radii for non-polar protein atoms were scaled by a factor of 0.8, while those for the ligands were not scaled. All compounds selected from the database by the similarity search were docked and scored using the Glide standard-precision (SP) mode. The top ranked compounds obtained in this way were redocked and rescored using the Glide extra-precision (XP) mode.

Post-Scoring with MM-GB/SA

The calculation of binding affinities using molecular mechanics and a continuum solvation model was introduced by Kuhn and Kollman using PB/SA to represent the solvent.⁴⁹ Since then, several modifications of this procedure have appeared in the literature.⁵⁰ In our version, a conformational search for the molecules in the unbound state and energy minimization for the complexes using OPLS-AA and GB/SA⁵¹ within Macromodel⁵² were performed. In the unbound state, all conformers within 5.0 kcal/mol of the lowest-energy conformer were retained. A root-mean-square deviation (RMSd) value of 0.3 Å for heavy atoms and hydrogens connected to heteroatoms was used to obtain unique conformations. Assuming a Boltzmann distribution, the probabilities for each conformer (P_i) were calculated and the average intramolecular and hydration energies for each compound obtained. The conformational entropies (S_{conf}) were calculated from the probabilities using eq 3, where k_B is the Boltzmann constant.

$$S_{conf} = -k_B \sum_{i=1}^n P_i \ln P_i \quad (3)$$

To better account for the protein flexibility, the best pose for a selected molecule was energy-minimized in the bound state. In the energy minimization, no constraints were applied to residues within 5 Å from a point near the center of the binding site. A second shell of 3 Å around the first shell was defined and constraints of 50 kcal/mol·Å² applied to the residues therein. The remaining residues were held fixed. The application of constraints during the energy minimization step is very important to reduce the noise in the protein energy values (E_{PTN}). Besides the protein energies, the energy-minimized structures for the complexes provided the intramolecular and solvation energies for the ligands in the protein environment, and the van der Waals (E_{VDW}) and electrostatic (E_{Elect}) interaction energies. In the bound state, it was assumed that there is only one conformation accessible to each ligand; its conformational entropy is therefore zero. This approximation should be revisited, though it may require a conformational search in the bound state. In this manner, the binding energy (ΔG_{bind}) was calculated by eq 4.

$$\Delta G_{bind} = \Delta E_{intra} + \Delta E_{solv} - T \Delta S_{conf} + E_{VDW} + E_{Elect} + E_{PTN} \quad (4)$$

In eq 4, ΔE_{intra} and ΔE_{solv} are the intramolecular and desolvation penalties for each ligand upon binding, obtained by the difference between these quantities in the bound and unbound states. ΔS_{conf} is the conformational entropy penalty, which is multiplied by the temperature to convert it into free energy. The final ranking was obtained by calculating relative binding energies ($\Delta \Delta G_{bind}$) using a NNRTI as reference (see below).

Results and Discussion

Chemical Similarity Search

Four different solutions that maximize the Euclidean and Tanimoto enrichment factors simultaneously were obtained. All of them retrieved well the known NNRTIs in the top 5% molecules (ca. 3500 molecules), specifically 62% and 54% for the Euclidean and Tanimoto coefficients, respectively. In each solution, the Euclidean and Tanimoto coefficients have identical sets of descriptors, whereas the descriptors for the first are weighted. MW (molecular weight), FOSA (the hydrophobic component of the total solvent accessible surface area (SASA)), FISA (the hydrophilic component of SASA), and HB donor (number of hydrogen bonds donated by the solute to water molecules), appear in all solutions. HB acceptor (number of hydrogen bonds accepted by the solute from water molecules), polarizability, and QPlogS (predicted aqueous solubility) occur in three solutions, while SASA and EA (PM3 calculated electron affinity) are in two and one solutions. A total of 1856 molecules, compounds that ranked among the top 2500 molecules in all solutions, together with 9 NNRTIs designed by our group and 26 other known NNRTIs (Figure 1), were docked in the binding sites of the wild-type and K103N enzymes.

Validation of the docking method

To ensure that the ligand orientations and positions obtained from the docking calculations were likely to represent reasonable binding modes for the compounds analyzed, nine NNRTIs complexed to HIV-RT for which either crystal structures or theoretical models are available were used to validate the Glide 3.5 XP function. The NNRTIs selected for our test calculations are TMC-125, DPC-083, S-DABO-3w, Sustiva (efavirenz), UC-781, MKC-442, loviride (alpha-APA), 9-CI-TIBO and nevirapine. No crystal structure for the inhibitors TMC-125, DPC-083, and S-DABO-3w complexed to HIV-RT are available. The complexes obtained from the docking calculations in these cases were compared to theoretical models previously suggested by our group for the first two compounds^{53,54} and to a docking study performed by Mai *et al.* for the last.⁵⁵

The experimental binding conformations for Sustiva, UC-781, MKC-442, loviride (alpha-APA), 9-Cl-TIBO and nevirapine agree very well with the conformations obtained by docking into the 1rt4 HIV-RT binding site. The RMSd between the predicted and the observed X-ray conformation for five of the NNRTIs is less than 1.0 Å (Figure 2). The only exception is 9-Cl-TIBO. The larger RMSd value in this case can be attributed to the different position for the methyl group attached to the seven-membered ring and to the orientation of the flexible 3,3-dimethylallyl group.

The docked structures for TMC-125, DPC-083 and SDABO-3w are shown in Figure 3. As in the theoretical models previously reported, the inhibitors display the characteristic hydrogen bonds with the backbone oxygen and nitrogen atoms of Lys101. Hydrophobic interactions with the arene pocket formed by the residues Tyr181, Tyr188, Phe227 and Trp229 were also reproduced as well as the interactions with the pocket formed by Leu234 and Tyr318.

Docking into the Wild-Type Reverse Transcriptase and Post-Scoring with MM-GB/SA

After this validation, the docking was extended to the 1856 compounds selected from the similarity search and the known NNRTIs. The Glide SP function was used as a filter to eliminate the least promising molecules. The top 500 compounds from the SP scoring were then redocked and rescored using the Glide XP function. Finally, the top 100 compounds were post-scored with MM-GB/SA. According to the docking score, 15 of the 35 known NNRTIs are among the top 100 compounds: S-DABO-3w (#1), TMC-125 (#4), DPC-083 (#11), DPC-961 (#12), Sustiva (#15), DPC-24 (#36), DPC-963 (#58), UC-781 (#62), MKC-442 (#71)), and 6 of the 9 compounds from our group, 23o (#2), 23n (#6), 23p (#7), 23j (#9), 23d (#10), and 23h (#28).^{43b} The remaining molecules are from the Maybridge database. Although loviride, 9-Cl-TIBO, and nevirapine are not among the first 100 compounds, they were also included in the post-scoring analysis because Glide reproduced their experimental binding modes very well (Figure 2).

Although more computationally demanding, the MM-GB/SA scoring gives far superior correlations with experimental activity data than standard docking scoring functions, as reported in the literature.⁵⁰ In our own experience, the MM-GB/SA methodology has, in general, also been much more reliable than docking for rank-ordering.⁵⁶ The final MM-GB/SA ranking was obtained by calculating relative binding energies ($\Delta\Delta G_{bind}$) using S-DABO-3w, the ligand with the most favorable binding energy, as reference. Figure 4 shows that the MM-GB/SA scoring yields a very good correlation with the biochemical assay data for S-DABO-3w, TMC-125, DPC-083, DPC-961, Sustiva, DPC-963, UC-781, MKC-442, loviride, 9-Cl-TIBO, and nevirapine.⁵⁷ Notably, a similar result was obtained with the Glide XP function. This might be associated with the relative rigidity of these molecules; the desolvation and intramolecular strain penalties for more flexible ligands can be expected to show greater variation. Though Glide works well for this subset of inhibitors, Figure 5 shows poor correlation between the scores obtained by Glide and MM-GB/SA for the top 100 compounds. Since this set contains more flexible analogs, the deficiencies of the docking function are amplified. For example, the compounds NRB00180, RJC03153, SP01208, S09268, RJC01037, and HTS02435 rank among the top 20 according to Glide. Once they are post-scored with MM-GB/SA, they are moved to the bottom of the list because of desolvation and intramolecular penalties of 8–11 kcal/mol and 7–17 kcal/mol, respectively. For example, the first four have a cis conformation for amides that is not penalized enough by the docking method. For comparison, S-DABO-3w has desolvation and intramolecular penalties of 3.6 and 0.8 kcal/mol.

The MM-GB/SA results for the top 20 compounds are listed in Table 1. Seven of the compounds are well-known NNRTIs, S-DABO-3w, TMC-125, UC-781, DPC-963, DPC-961, efavirenz, and DPC-24. Loviride, DPC-083, nevirapine, 9-Cl-TIBO, and MKC-442 scored less well,

ranking #40, #41, #52, #53, and #60, respectively. Comparing to S-DABO-3w, loviride has a greater desolvation penalty, nevirapine and MKC-442 have poorer electrostatic complementarity with the enzyme, DPC-083 has poorer VDW interactions, and 9-Cl-TIBO has both larger intramolecular penalty and poorer interactions. The analysis of the contributions to $\Delta\Delta G_{bind}$ for the top-scoring NNRTIs shows that they bind well to HIV-RT due to very favorable interactions with the enzyme for TMC-125, UC-781, and DPC-24, and because of small intramolecular and desolvation penalties for the more rigid DPC-963, DPC-961, and Sustiva. SDABO-3w is the best ranking NNRTI according to the calculations because it combines favorable interactions with small intramolecular and desolvation penalties.

As shown in Table 1 and Figure 6, 10 of the first 20 compounds are from the Maybridge database: S10087, NRB03328, KM06633, KM06632, NRB03323, KM06631, NRB03309, NRB03321, NRB03310, and NRB03324. S10087 is the only one of its class that is among the top 20, although the closely related analogs S10089, S10085, and S10076 rank very well, #21, #26, and #35. KM06631 and KM06632 are analogs of KM06633, while NRB03323, NRB03309, NRB03321, NRB03310, and NRB03324 are analogs of NRB03328. It is notable that Muraglia and co-workers recently reported a series of aryltetrazolylacetanilides, structurally similar to NRB03328 and analogs, with very good potency against HIV-RT.⁵⁸ The analysis of the contributions to $\Delta\Delta G_{bind}$ shows that the van der Waals interactions and the entropy penalty term are comparable for S-DABO-3w and the top scoring compounds from the database. It also shows that S10087, NRB03328, KM06633, and analogs yield minimal protein deformation; E_{PTN} is ca. -953.0 kcal/mol compared to -947.3 kcal/mol for SDABO-3w. On the other hand, the small protein deformations for these compounds are partially offset by greater desolvation and intramolecular penalties; S10087, NRB03328, KM06633, and analogs have combined desolvation and intramolecular penalties ranging from 6.0 to 12.0 kcal/mol, while the value for SDABO-3w is 4.4 kcal/mol. As for the electrostatic interactions with HIV-RT, the values are ca. -14.0 kcal/mol for NRB03328, KM06633, and analogs, compared to -20.4 and -17.9 kcal/mol for S10087 and S-DABO-3w, respectively.

Figure 7 illustrates the complexes between HIV-RT and S10087, NRB03328, and KM06633. The top compounds from the database are predicted to bind to HIV-RT in a very similar manner to known NNRTIs. S10087 and KM06633 display simultaneous hydrogen bonds with the backbone oxygen and nitrogen atoms of Lys101, while NRB03328 forms a single hydrogen bond with the backbone oxygen of Lys101. These compounds also form hydrophobic interactions with the arene pocket (Tyr181, Tyr188, Phe227 and Trp229) and with the pocket formed by Leu234 and Tyr318.

Previous analyses by our group pointed to the Het-NH-Ph-U class as promising NNRTIs, where Het is an aromatic heterocycle and U is an unsaturated hydrophobic group.^{43a} Thus, compounds with Het = 2-thiazoyl and 2-pyrimidinyl were synthesized and assayed for anti-viral activity. Nine of them were docked to HIV-RT, six 2-pyrimidinyl and three 2-thiazoyl derivatives. The thiazoles did not survive the docking filter, while all of the 2-pyrimidinyl compounds appeared among the best 100 candidates. Our previous findings also showed that the pyrimidines are generally more active than the thiazoles.^{43a} Post-scoring with MM-GB/SA resulted in three of the pyrimidines ranking among the top 20 as shown in Table 1 and Figure 6 (23p, 23h, and 23o). The other three, 23n, 23d, and 23j, ranked #25, #32, and #43. The contributions to $\Delta\Delta G_{bind}$ are equivalent for the top scoring 2-pyrimidines and S-DABO-3w, particularly the protein deformation and van der Waals interactions. The more favorable binding of SDABO-3w can be attributed to smaller desolvation and intramolecular penalties. The combined penalty for S-DABO-3w is 4.4 kcal/mol, while it is 9.6, 7.6, and 10.5 kcal/mol for 23p, 23h, and 23o. The amino group in 23p and 23o is responsible for the larger desolvation and intramolecular penalties, but provides a more favorable electrostatic interaction with the enzyme due to hydrogen bonding with the Glu138 carboxylate group.

The complexes for the best scoring 2-pyrimidines are shown in Figure 8a; they are completely consistent with what we have obtained previously using the BOMB ligand-growing program and Monte Carlo simulations.⁴³ A pyrimidine and the diarylamino nitrogen are hydrogen bonded to the backbone nitrogen and oxygen atoms of Lys101, the phenyl ring is interacting with Leu234 and Tyr318, and the 3,3-dimethylallyloxy group is in the arene pocket. This pocket is occupied by such unsaturated groups for most NNRTIs, e.g., in Figures 2, 3, and 8b.

Docking into the K103N Reverse Transcriptase and Post-Scoring with MM-GB/SA

The top 100 compounds ranked by the Glide XP function after docking with K103N-RT were post-scored with MM-GB/SA. The top 20 compounds after the MM-GB/SA scoring are displayed in Figure 9. The results for the mutant show that 9 well-known NNRTIs scored among the first 20 (DPC-24 (#5), DPC-27 (#6), TMC-125 (#8), 6-FQXPT (#9), DPC-963 (#10), 2-methyl-nevirapine (#11), S-DABO-3w (#12), 8-CI-TIBO (#14), and DPC-961 (#15)). Other post-scored NNRTIs were Sustiva (#21), nevirapine (#25), loviride (#31), delavirdine (#33), 4-methyl-MBI (#34), DPC-083 (#37), PNU-32945 (#78), and MKC-442 (#95). Of those, it is known that the activities for DPC-961, DPC-963, TMC-125, and S-DABO-3w against the K103N mutant are moderately reduced, while other NNRTIs like loviride, Sustiva, nevirapine, delavirdine, MKC-442, and 6-FQXPT are more adversely affected by this specific mutation.⁵⁹

It has been suggested elsewhere that the K103N mutation hampers the binding and confers resistance to many classes of NNRTIs because of enhanced stabilization of the unliganded state; this stabilization is derived from a hydrogen bond between the Asn103 and Tyr188 side chains.⁶⁰ Thus, in order to compensate for the loss of this hydrogen bond in the bound state, the design of compounds that specifically interact with Asn103 is desirable. A carbonyl in the inhibitor seems preferred to target the K103N mutant as it can accept simultaneous hydrogen bonds from the Lys101 backbone and Asn103 side-chain NH groups. Most of the top-scoring NNRTIs (DPC-24, DPC-27, DPC-961, DPC-963, SDABO-3w, and Sustiva) have a carbonyl group that interacts with both residues.

The compounds from the Maybridge database that ranked among the best 20 for the mutant are HTS03792 (#7), RJF01584 (#13), KM06633 (#16), NRB02128 (#17), RJC03349 (#18), HTS02435 (#19), and RJC03153 (#20). Thus, the only one that scored well for both the wild-type and K103N forms was KM06633. This compound also has a carbonyl group that interacts with Lys101 and Asn103. Although analogs of KM06633 like KM06623, KM06632, and KM06631 are not among the top 20 for K103N-RT, they also ranked well, i.e., #22, #28, and #35. Analogs of S10087 and NRB03328 did not survive the docking filter except for S10085. Figure 10 shows the computed complexes for K103N-RT with S-DABO-3w, DPC-963, and KM06633.

The amino-pyrimidines 23o, 23n, 23p, and 23j are the best ligands for the mutant according to MM-GB/SA. The mono-substituted pyrimidine analog 23h lacking the amino group did not survive the docking filter. A practical problem with these amino derivatives is that they turned out to be relatively cytotoxic, e.g., 23n and 23o have CC₅₀ values of 2 and 55 nM, while this is not a problem for methoxy analog 23h, which has EC₅₀ and CC₅₀ values of 10 nM and 9 μM in the wild-type assay.^{43b,c} Figure 10 illustrates the complex between 23o and K103N-RT. In the mutant, one of the pyrimidine nitrogens accepts a hydrogen bond from the Asn103 side-chain, even though the directionality for this interaction is not optimal. The pyrimidine and the diarylamino nitrogens are hydrogen bonded to the backbone nitrogen and oxygen atoms of Lys101, while the amino group is hydrogen bonded to Glu138. The amino-pyrimidines bind to both the mutant and the wild-type enzymes in a very similar manner. This contrasts with TMC-125. For HIV-RT, TMC-125 interacts simultaneously with Lys101 and Glu138. In the mutant, however, the less flexible TMC-125 is shifted in the pocket and establishes new

interactions. The predicted binding mode agrees with the one displayed in the X-ray structure for TMC-125 complexed with the K103N mutant (PDB ID: 1sv5). The pyrimidine and the diarylamino nitrogens are now hydrogen bonded to the backbone nitrogen and oxygen atoms of Lys102, while the amino group of TMC-125 is no longer hydrogen bonded to Glu138. In spite of that, the activity of TMC-125 is not significantly affected by the K103N mutation.³⁵

Assay Results and Modifications of S10087

Six of the top-20 library compounds from Figure 6 were purchased from Maybridge: S10087, KM06631, KM06632, KM06633, NRB03321, and NRB03323. Many of the other high-ranking library compounds were in these series including the four additional NRB compounds in Figure 6 and three analogs of S10087, which differ by replacement of the 4-methyl group with 3-fluoro (S10076), 3-chloro, 4-methyl (S10085), and 2,4-dichloro (S10089). The two purchased NRB compounds were impure and gave incorrect mass spectra. The other four gave correct NMR and mass spectra. After purification, they were submitted to an anti-HIV assay using infected human T-cells, but they failed to inhibit HIV replication in the MT-2 cells at concentrations up to 100 μ M.

The lack of activity might have several sources. (1) The library with ca. 70,000 members is not large, though known actives were retrieved well by the MM-GB/SA protocol, and library compounds were interspersed with the known actives. (2) There is high sensitivity of activity to structure for HIV-RT inhibitors;⁴³ for example, the core may be viable, but the substituents may be not quite right. The assay was only run to 100 μ M. Though some compounds might show activity at higher concentrations, 100 μ M is often a practical limit owing either to solubility of the compounds or their cell-toxicity. For example, the CC_{50} values for S10087, KM06631, KM06632, and KM06633 are 61, 41, 75, and 3 μ M with the MT-2 cells. (3) Perhaps more compounds should have been purchased, “digging deeper into the deck”. In fact, 16 compounds had been purchased from Maybridge and assayed from a preliminary version of the same docking exercise that did not include the MM-GB/SA post-scoring. This included KM06633, and HTS02435 and RJC03153 from Figure 9. All 16 compounds were purified and characterized by NMR and mass spectrometry, and all were found to be inactive in the MT-2 assay. Structure visualization indicated that there were generousities in the evaluation of conformational energetics by *Glide* including some twisted groups such as amides that should be more-or-less planar, which led to the development and application of the present MM-GB/SA post-scoring.

Thus, we then chose to focus on the oxadiazole lead, which ranked third in Figure 6, as a possible near-miss. A limited substituent scan was performed for the anilinybenzyloxadiazole core with the BOMB program,^{43a} which creates analogs from a core that has been placed in the binding site. The computational analysis suggested removal of the methoxy groups in the benzyl ring and addition of smaller, more hydrophobic groups to the aniliny and benzyl rings like chlorine and methyl. Subsequent synthesis and assaying of several polychloro-analogs yielded anti-HIV agents with EC_{50} values as potent as 310 nM in the wild-type MT-2 cell assay, as illustrated for the analog JL0203 in Figure 11. Nevirapine yields an EC_{50} of 110 nM in the same assay. Full details of these experimental studies are provided elsewhere.⁶¹ Thus, the docking exercise was unsuccessful in directly delivering active compounds from the Maybridge library. However, it was provocative and did lead to a novel NNRTI core that has now been demonstrated to be viable with the aid of synthetic chemistry.

Conclusions

A chemical similarity search on the Maybridge database was performed by *QikSim* using known non-nucleoside inhibitors of the HIV-1 reverse transcriptase as reference structures in order to identify potentially active compounds. The top ranked molecules obtained from this

procedure and 35 known NNRTIs were docked into the binding sites of both the wild-type RT (HIV-RT) and its K103N variant (K103N-RT) using Glide 3.5. The docking method provided good agreement between the binding poses and X-ray structures or theoretical models available for the complexes between HIV-RT and nine NNRTIs. The top 100 compounds ranked by Glide XP after docking into the binding pockets of HIV-RT and K103N-RT were post-scored with molecular mechanics and continuum solvation (MM-GB/SA). Three NNRTIs (23p, 23h, and 23o) from our group, seven other known NNRTIs (S-DABO-3w, TMC-125, UC-781, DPC-963, DPC-961, Sustiva, and DPC-24) and 10 compounds from the database (S10087, KM06633, KM06631, KM06632, NRB03328, NRB03323, NRB03309, NRB03321, NRB03310, and NRB03324) appeared among the top 20 ligands for HIV-RT. The results were encouraging as Muraglia and co-workers recently reported a series of aryltetrazolylacetanilides, structurally similar to NRB03328 and its top scoring analogs, with good potency against HIV-RT.⁵⁸ The viability of the present approach is further supported by the results obtained for K103N-RT. The NNRTIs S-DABO-3w, TMC-125, DPC-961, and DPC-963, which are known to retain activity well against the K103N mutant, also scored among the best 20 in this ranking. However, purchase and assaying of representative, top-scoring compounds from the Maybridge library failed to yield active anti-HIV agents. As HIV-RT is a target known to be very sensitive to the ligand's substituent pattern, S10087 was subjected to further computational analysis to seek modifications that would potentially provide a true active. Subsequent synthesis and assaying revealed that S10087 was in fact a "near-miss" since several closely related analogs were found to be potent anti-HIV agents. Thus, with the aid of computational tools, it was possible to evolve a false positive from the virtual screening into a true active.

Acknowledgements

Gratitude is expressed to the National Institutes of Health (GM32136) and National Institutes of Allergy and Infective Diseases (AI44616) for support of this research.

References

1. 2006 AIDS Epidemic Update. UNAIDS; Geneva: 2006.
2. De Clercq E. New anti-HIV agents and targets. *Med. Res. Rev* 2002;22:531–565. [PubMed: 12369088]
3. Katz RA, Skalka AM. The Retroviral Enzymes. *Annu. Rev. Biochem* 1994;63:133–173. [PubMed: 7526778]
4. Tantillo C, Ding J, Jacobo-Molina A, Nanni RG, Boyer PL, Hughes SH, Pauwels R, Andries K, Janssen PAJ, Arnold E. Locations of anti-AIDS drug binding sites and resistance mutations in the three-dimensional structure of HIV-1 reverse transcriptase: implications for mechanisms of drug inhibition and resistance. *J Mol Biol* 1994;243:369–387. [PubMed: 7525966]
5. Kohlstaedt LA, Wang J, Friedman JM, Rice PA, Steitz TA. Crystal structure at 3.5 Å resolution of HIV-1 reverse transcriptase complexed with an inhibitor. *Science* 1992;256:1783–1790. [PubMed: 1377403]
6. Smerdon SJ, Jager J, Wang J, Kohlstaedt LA, Chirino AJ, Friedman JM, Rice PA, Steitz TA. Structure of the binding site for nonnucleoside inhibitors of reverse transcriptase of human immunodeficiency virus type 1. *Proc. Natl. Acad. Sci* 1994;91:3911–3915. [PubMed: 7513427]
7. Ren JS, Esnouf R, Garman E, Somers D, Ross C, Kirby I, Keeling J, Darby G, Jones Y, Stuart D, Stammers D. High resolution structures of HIV-1 RT from four RT-inhibitor complexes. *Nature Struct. Biol* 1995;2:293–302. [PubMed: 7540934]
8. Ren J, Esnouf R, Hopkins A, Ross C, Jones Y, Stammers D, Stuart D. The structure of HIV-1 reverse-transcriptase complexed with 9-chloro-TIBO - Lessons for inhibitor design. *Structure* 1995;3:915–926. [PubMed: 8535785]
9. Hopkins AL, Ren JS, Esnouf RM, Willcox BE, Jones EY, Ross C, Miyasaka T, Walker RT, Tanaka H, Stammers DK, Stuart DI. Complexes of HIV-1 reverse transcriptase with inhibitors of the HEPT

- series reveal conformational changes relevant to the design of potent nonnucleoside inhibitors. *J. Med. Chem* 1996;39:1589–1600. [PubMed: 8648598]
10. Esnouf RM, Ren J, Hopkins AL, Ross CK, Jones EY, Stammers DK, Stuart DI. Unique features in the structure of the complex between HIV-1 reverse transcriptase and the bis(heteroaryl)piperazine (BHAP) U-90152 explain resistance mutations for this nonnucleoside inhibitor. *Proc. Natl. Acad. Sci. U.S.A* 1997;94:3984–3989. [PubMed: 9108091]
 11. Hsiou Y, Das K, Ding J, Clark AD Jr, Kleim JP, Rosner M, Winkler I, Riess G, Hughes SH, Arnold E. Structures of Tyr188Leu mutant and wild-type HIV-1 reverse transcriptase complexed with the non-nucleoside inhibitor HBY 097: inhibitor flexibility is a useful design feature for reducing drug resistance. *J. Mol. Biol* 1998;284:313–323. [PubMed: 9813120]
 12. Ren J, Esnouf RM, Hopkins AL, Warren J, Balzarini J, Stuart DI, Stammers DK. Crystal structures of HIV-1 reverse transcriptase in complex with carboxanilide derivatives. *Biochemistry* 1998;37:14394–14403. [PubMed: 9772165]
 13. Ren J, Esnouf RM, Hopkins AL, Stuart DI, Stammers DK. Crystallographic analysis of the binding modes of thiazoloisoindolinone non-Nucleoside inhibitors to HIV-1 reverse transcriptase and comparison with modeling studies. *J. Med. Chem* 1999;42:3845–3851. [PubMed: 10508433]
 14. Ren J, Milton J, Weaver KL, Short SA, Stuart DI, Stammers DK. Structural basis for the resilience of efavirenz (DMP-266) to drug resistance mutations in HIV-1 reverse transcriptase. *Structure* 2000;8:1089–1094. [PubMed: 11080630]
 15. Ren J, Nichols C, Bird LE, Fujiwara T, Sugimoto H, Stuart DI, Stammers DK. Binding of the second generation non-nucleoside inhibitor S-1153 to HIV-1 reverse transcriptase involves extensive main chain hydrogen bonding. *J. Biol. Chem* 2000;275:14316–14320. [PubMed: 10799511]
 16. Ren J, Diprose J, Warren J, Esnouf RM, Bird LE, Ikemizu S, Slater M, Milton J, Balzarini J, Stuart DI, Stammers DK. Phenylethylthiazolylthiourea (PETT) non-nucleoside inhibitors of HIV-1 and HIV-2 reverse transcriptases. Structural and biochemical analysis. *J. Biol. Chem* 2000;275:5633–5639. [PubMed: 10681546]
 17. Hogberg M, Sahlberg C, Engelhardt P, Noreen R, Kangasmetsa J, Johansson NG, Oberg B, Vrang L, Zhang H, Sahlberg BL, Unge T, Lovgren S, Fridborg K, Backbro K. Urea-PETT compounds as a new class of HIV-1 reverse transcriptase inhibitors. 3. Synthesis and further structure-activity relationship studies of PETT analogues. *J. Med. Chem* 2000;43:304–304. [PubMed: 10650066]
 18. Chan JH, Hong JS, Hunter RN III, Orr GF, Cowan JR, Sherman DB, Sparks SM, Reitter BE III, Andrews CW III, Hazen RJ, St Clair M, Boone LR, Ferris RG, Creech KL, Roberts GB, Short SA, Weaver K, Ott RJ, Ren J, Hopkins A, Stuart DI, Stammers DK. 2-Amino-6-arylsulfonylbenzotrioles as non-nucleoside reverse transcriptase inhibitors of HIV-1. *J. Med. Chem* 2001;44:1866–1882. [PubMed: 11384233]
 19. Ding J, Das K, Moereels H, Koymans L, Andries K, Janssen PAJ, Hughes SH, Arnold E. Structure of HIV-1/TIBO R86183 complex reveals similarity in the binding of diverse nonnucleoside inhibitors. *Mat. Struct. Biol* 1995;2:407–415.
 20. De Clercq E. Non-nucleoside reverse transcriptase inhibitors (NNRTIs) for the treatment of human immunodeficiency virus type 1 (HIV-1) infections: strategies to overcome drug resistance development. *Med. Res. Rev* 1996;16:125–157. [PubMed: 8656777]
 21. Tanaka H, Takashima H, Ubasawa M, Sekiya K, Inouye N, Baba M, Shigeta S, Walker RT, De Clercq E, Miyasaka T. Synthesis and antiviral activity of 6-benzyl analogs of 1-[(2-hydroxyethoxy)methyl]-5-(phenylthio)thymine (HEPT) as potent and selective anti-HIV-1 agents. *J. Med. Chem* 1995;38:2860–2865. [PubMed: 7636846]
 22. Pauwels R, Andries K, Desmyter J, Schols D, Kukla MJ, Breslin HJ, Raeymaeckers A, Van Gelder J, Woestenborghs R, Heykants J, Schellekens K, Janssen MAC, De Clercq E, Janssen PAJ. Potent and selective inhibition of HIV-1 replication *in vitro* by a novel series of TIBO derivatives. *Nature* 1990;343:470–473. [PubMed: 1689015]
 23. Kukla MJ, Breslin HJ, Pauwels R, Fedde CL, Miranda M, et al. Synthesis and anti-HIV-1 activity of 4,5,6,7-tetrahydro-5-methylimidazo[4,5,1-jk][1,4]benzodiazepin-2(1H)-one (TIBO) derivatives. *J. Med. Chem* 1991;34:746–751. [PubMed: 1995896]
 24. Goldman ME, Nunberg JH, O'Brien JA, Quintero JC, Schleif WA, Freund KF, Gaul SL, Saari WS, Wai JS, Hoffman JM, Anderson PS, Hupe DJ, Emini EA, Stern AM. Pyridinone derivatives: Specific

- human immunodeficiency virus type 1 reverse transcriptase inhibitors with antiviral activity. *Proc. Natl. Acad. Sci. U.S.A* 1991;88:6863–6867. [PubMed: 1713693]
25. Pauwels R, Andries K, Debyser Z, Van Daele P, Schols D, Stoffels P, De Vreese K, Woestenborghs R, Vandamme A-M, Janssen CGM, Anné J, Cauwenbergh G, Desmyter J, Heykants J, Janssen MAC, De Clercq E, Janssen PAJ. Potent and highly selective human immunodeficiency virus type 1 (HIV-1). Inhibition by a series of α -anilinophenylacetamide derivatives targeted at HIV-1 reverse transcriptase. *Proc. Natl. Acad. Sci. U.S.A* 1993;90:1711–1715. [PubMed: 7680476]
 26. Fujiwara T, Sato A, el-Farrash M, Miki S, Abe K, Isaka Y, Kodama M, Wu Y, Chen LB, Harada H, Sugimoto H, Hatanaka M. S-1153 inhibits replication of known drug-resistant strains of human immunodeficiency virus type 1. *Antimicrob. Agents Chemother* 1998;42:1340–1345. [PubMed: 9624472]
 27. Ahgren C, Backro K, Bell FW, Cantrell AS, Clemens M, Colacino JM, Deeter JB, Engelhardt JA, Högberg M, Jaskunas SR, Johansson NG, Jordan CL, Kasher JS, Kinnick MD, Lind P, Lopez C, Morin JM Jr, Muesing MA, Noreen R, Öberg B, Paget CJ, Palkowitz JA, Parrish CA, Pranc P, Rippey MK, Rydergard C, Sahlberg C, Swanson S, Ternansky RJ, Unge T, Vasileff RT, Vrang L, West SJ, Zhang H, Zhou X-X. The PETT series, a new class of potent nonnucleoside inhibitors of human immunodeficiency virus type 1 reverse transcriptase. *Antimicrob. Agents Chemother* 1995;39:1329–1335. [PubMed: 7574525]
 28. Högberg M, Sahlberg C, Engelhardt P, Noreen R, Kangasmetsa J, Johansson NG, Öberg B, Vrang L, Zhang H, Sahlberg BL, Unge T, Lövgren S, Fridborg K, Backbrö K. Urea-PETT compounds as a new class of HIV-1 reverse transcriptase inhibitors. 3. Synthesis and further structure-activity relationship studies of PETT analogues. *J. Med. Chem* 1999;42:4150–4160. [PubMed: 10514285]
 29. Baba S, Shigeta S, Yuasa, Takashima H, Sekiya K, Ubasawa M, Tanaka H, Miyasaka T, Walker RT, De Clercq E. Preclinical evaluation of MKC-442, a highly potent and specific inhibitor of human immunodeficiency virus type 1 in vitro. *Antimicrob. Agents Chemother* 1994;38:688–692. [PubMed: 7518216]
 30. Corbett JW, Ko SS, Rodgers JD, Jeffrey S, Bachelier LT, Klabe RM, Diamond S, Lai CM, Rabel SR, Saye JA, Adams SP, Trainor GL, Anderson PS, Erickson-Viitanen SK. Expanded-spectrum nonnucleoside reverse transcriptase inhibitors inhibit clinically relevant mutant variants of human immunodeficiency virus type 1. *Antimicrob. Agents Chemother* 1999;43:2893–2897. [PubMed: 10582878]
 31. Campiani G, Aiello F, Fabbrini M, Morelli E, Ramunno A, Armaroli S, Nacci V, Garofalo A, Greco G, Novellino E, Maga G, Spadari S, Bergamini A, Ventura L, Bongiovanni B, Capozzi M, Bolacchi F, Marini S, Coletta M, Guiso G, Caccia S. Quinoxalinyethylpyridylthioureas (QXPTs) as potent non-nucleoside HIV-1 reverse transcriptase (RT) inhibitors. Further SAR studies and identification of a novel orally bioavailable hydrazine-based antiviral agent. *J. Med. Chem* 2001;44:305–315. [PubMed: 11462972]
 32. Pani A, Musiu C, Loi AG, Mai A, Loddo R, La Colla P, Marongiu ME. DABOs as candidates to prevent mucosal HIV transmission. *Antiviral Chem. Chemother* 2001;12:51–59.
 33. Esnouf RM, Stuart DI, De Clercq E, Schwartz E, Balzarini J. Models which explain the inhibition of reverse transcriptase by HIV-1 specific (thio)carboxanilide derivatives. *Biochem. Biophys. Res. Commun* 1997;234:458–464. [PubMed: 9177293]
 34. Andries K, Azijn H, Thielemans T, Ludovici D, Kukla M, Heeres J, Janssen P, De Corte B, Vingerhoets J, Pauwels R, Béthune M. TMC125, a novel next-generation nonnucleoside reverse transcriptase inhibitor active against nonnucleoside reverse transcriptase inhibitor-resistant human immunodeficiency virus type 1. *Antimicrob. Agents Chemother* 2004;48:4680–4686. [PubMed: 15561844]
 35. Das K, Clark AD Jr, Lewi PJ, Heeres J, De Jonge MR, et al. Roles of conformational and positional adaptability in structure-based design of TMC125-R165335 (etravirine) and related nonnucleoside reverse transcriptase inhibitors that are highly potent and effective against wild-type and drug-resistant HIV-1 variants. *J. Med. Chem* 2004;47:2550–2560. [PubMed: 15115397]
 36. Bachelier L, Jeffrey S, Hanna G, D'Aquila R, Wallace L, Logue K, Cordova B, Hertogs K, Larder B, Buckery R, Baker D, Gallagher K, Scarnati H, Tritch R, Rizzo C. Genotypic correlates of phenotypic resistance to efavirenz in virus isolates from patients failing nonnucleoside reverse transcriptase inhibitor therapy. *J. Virol* 2001;75:4999–5008. [PubMed: 11333879]

37. Richmand DD, Havlir D, Corbeil J, Looney D, Ignacio C, Spector SA, Sullivan J, Cheeseman S, Barringer K, Pauletti D, Shih CK, Myers M, Griffin J. nevirapine resistance mutations of human-immunodeficiency-virus type 1 selected during therapy. *J. Virol* 1994;68:1660–1666. [PubMed: 7509000]
38. Corbett JW, Ko SS, Rodgers JD, Gearhart LA, Magnus NA, Bachelier LT, Diamond S, Jeffrey S, Klabe RM, Cordova BC, Garber S, Logue K, Trainor GL, Anderson PS, Erickson-Viitanen SK. Inhibition of clinically relevant mutant variants of HIV-1 by quinazolinone non-nucleoside reverse transcriptase inhibitors. *J. Med. Chem* 2000;43:2019–2030. [PubMed: 10821714]
39. Willett P, Barnard JM, Downs GM. Chemical Similarity Searching. *J. Chem. Inf. Comput. Sci* 1998;38:983–996.
40. Maggiora, GM.; Johnson, MA. *Concepts and Applications of Molecular Similarity*. John Wiley & Sons; New York: 1990. p. 99–117.
41. Willett P. Similarity-based approaches to virtual screening. *Biochem. Soc. Trans* 2003;31:603–606. [PubMed: 12773164]
42. Su AI, Lorber DM, Weston GS, Baase WA, Matthews BW, Shoichet BK. Docking molecules by families to increase the diversity of hits in database screens: Computational strategy and experimental evaluation. *Proteins* 2001;42:279–293. [PubMed: 11119652]
43. a Jorgensen WL, Ruiz-Caro J, Tirado-Rives J, Basavapathruni A, Anderson KS, Hamilton AD. Computer-aided design of non-nucleoside inhibitors of HIV-1 reverse transcriptase. *Bioorg. Med. Chem. Lett* 2006;16:663–667. [PubMed: 16263277] b Ruiz-Caro J, Basavapathruni A, Kim JT, Bailey CM, Wang L, Anderson KS, Hamilton AD, Jorgensen WL. Optimization of diarylamines as non-nucleoside inhibitors of HIV-1 reverse transcriptase. *Bioorg. Med. Chem. Lett* 2006;16:668–671. [PubMed: 16298131] c Thakur VV, Kim JT, Hamilton AD, Bailey CM, Domaoal RA, Wang L, Anderson KS, Jorgensen WL. Optimization of pyrimidinyl- and triazinyl-amines as non-nucleoside inhibitors of HIV-1 reverse transcriptase. *Bioorg. Med. Chem. Lett* 2006;16:5664–5667. [PubMed: 16931015] d Kim JT, Hamilton AD, Bailey CM, Domaoal RA, Wang L, Anderson KS, Jorgensen WL. FEP-guided selection of bicyclic heterocycles in lead optimization for non-nucleoside inhibitors of HIV-1 reverse transcriptase. *J. Am. Chem. Soc* 2006;128:15372–15373. [PubMed: 17131993]
44. QikProp, Version 2.3. Schrödinger, Inc.; New York: 2005. Jorgensen, WL. QikSim, Version 2.3. Yale University; New Haven, CT: 2005.
45. Jorgensen WL. The Many Roles of Computation in Drug Discovery. *Science* 2004;303:1813–1818. [PubMed: 15031495]
46. a Friesner RA, Banks JL, Murphy RB, Halgren TA, Klicic JJ, Mainz DT, Repasky MP, Knoll EH, Shelley M, Perry JK, Shaw DE, Francis P, Shenkin PS. Glide: A new approach for rapid, accurate docking and scoring. 1. Method and assessment of docking accuracy. *J. Med. Chem* 2004;47:1739–1749. [PubMed: 15027865] b Halgren TA, Murphy RB, Friesner RA, Beard HS, Frye LL, Pollard WT, Banks JL. Glide: A new Approach for rapid, accurate docking and scoring. 2. Enrichment factors in database screening. *J. Med. Chem* 2004;47:1750–1759. [PubMed: 15027866]
47. Jorgensen WL, Maxwell DS, Tirado-Rives J. Development and testing of OPLS all-atom force field on conformational energetics and properties of organic liquids. *J. Am. Chem. Soc* 1996;118:11225–11235.
48. Halgren TA. MMFF VII. Characterization of MMFF94, MMFF94s, and other widely available force fields for conformational energetics and for intermolecular interactions energies and geometries. *J. Comput. Chem* 1999;20:730–748.
49. Kuhn B, Kollman PA. Binding of a diverse set of ligands to avidin and streptavidin: An accurate quantitative prediction of their relative affinities by a combination of molecular mechanics and continuum solvent models. *J. Med. Chem* 2000;43:3786–3791. [PubMed: 11020294]
50. a Bernacki K, Kalyanaraman C, Jacobson MP. Virtual ligand screening against Escherichia coli dihydrofolate reductase: Improving docking enrichment physics-based methods. *J. Biomol. Screening* 2005;10:675–681. b Huang N, Kalyanaraman C, Irwin JJ, Jacobson MP. Physics-based scoring of protein-ligand complexes: Enrichment of known inhibitors in large-scale virtual screening. *J. Chem. Inf. Model* 2006;46:243–253. [PubMed: 16426060] c Huang N, Kalyanaraman C, Bernacki K, Jacobson MP. Molecular mechanics methods for predicting protein–ligand binding. *Phys. Chem. Chem. Phys* 2006;8:5166–5177. [PubMed: 17203140] d Lyne PD, Lamb ML, Saeh JC. Accurate

- prediction of the relative potencies of members of a series of kinase inhibitors using molecular docking and MM-GBSA scoring. *J. Med. Chem* 2006;49:4805–4808. [PubMed: 16884290]
51. Still WC, Tempczyk A, Hawley RC, Hendrickson T. A General treatment of solvation for molecular mechanics. *J. Am. Chem. Soc* 1990;112:6127.
 52. MacroModel, version 9.0. Schrödinger, LLC; New York, NY: 2005.
 53. Udier-Blagovic M, Tirado-Rives J, Jorgensen WL. Validation of a model for the complex of HIV-1 reverse transcriptase with nonnucleoside inhibitor TMC125. *J. Am. Chem. Soc* 2003;125:6016–6017.
 54. Udier-Blagovic M, Tirado-Rives J, Jorgensen WL. Structural and energetic analyses of the effects of the K103N mutation of HIV-1 reverse transcriptase on efavirenz analogues. *J. Med. Chem* 2004;47:2389–2392. [PubMed: 15084137]
 55. Mai A, Sbardella G, Artico M, Ragno R, Massa S, Novellino E, Greco G, Lavecchia A, Musiu C, La Colla M, Murgioni C, La Colla P, Loddo R. Structure-based design, synthesis, and biological evaluation of conformationally restricted novel 2-Alkylthio-6-[1-(2,6-difluorophenyl)alkyl]-3,4-dihydro-5-alkylpyrimidin-4(3H)-ones as non-nucleoside Inhibitors of HIV-1 reverse transcriptase. *J. Med. Chem* 2001;44:2544–2554. [PubMed: 11472208]
 56. In application of the Glide XP function negligible correlation was found with experimental data for congeneric series of 22 Factor Xa inhibitors, 28 CDK2 inhibitors, and 14 thrombin inhibitors, while the R^2 values obtained with the present MM-GB/SA scoring were 0.76, 0.69, and 0.81, respectively.
 57. a King RW, Klabe RM, Reid CD, Erickson-Viitanen SK. Potency of nonnucleoside reverse transcriptase inhibitors (NNRTIs) used in combination with other human immunodeficiency virus NNRTIs, NRTIs, or protease inhibitors. *Antimicrob. Agents Chemother* 2002;46:1640–1646. [PubMed: 12019069] b Mai A, Sbardella G, Artico M, Ragno R, Massa S, Novellino E, Greco G, Lavecchia A, Musiu C, La Colla M, Murgioni C, La Colla P, Loddo R. Structure-based design, synthesis, and biological evaluation of conformationally restricted novel 2-Alkylthio-6-[1-(2,6-difluorophenyl)alkyl]-3,4-dihydro-5-alkylpyrimidin-4(3H)-ones as non-nucleoside inhibitors of HIV-1 reverse transcriptase. *J. Med. Chem* 2001;44:2544–2554. [PubMed: 11472208] c Sahlberg C, Noréen R, Engelhardt P, Högberg M, Kangasmetsä J, Vrang L, Zhang H. Synthesis and anti-HIV activities of Urea-pETT analogs belonging to a new class of potent non-nucleoside HIV-1 reverse transcriptase inhibitors. *Bioorg. Med. Chem. Lett* 1998;8:1511–1516. [PubMed: 9873380] d Herrewewege YV, Michiels J, Van Roey J, Franssen K, Kestens L, Balzarini J, Lewi P, Vanham G, Janssen P. In Vitro evaluation of nonnucleoside reverse transcriptase inhibitors UC-781 and TMC120-R147681 as human immunodeficiency virus microbicides. *Antimicrob. Agents Chemother* 2004;48:337–339. [PubMed: 14693562] e De Clercq E. Perspectives of non-nucleoside reverse transcriptase inhibitors (NNRTIs) in the therapy of HIV-1 infection. *Farmacologia* 1999;54:26–45. [PubMed: 10321027]
 58. Muraglia E, Kinzel OD, Laufer R, Miller MD, Moyer G, Munshi V, Orvieto F, Palumbi MC, Pescatore G, Rowley M, Williams PD, Summa V. Tetrazole thioacetanilides: Potent non-nucleoside inhibitors of WT HIV reverse transcriptase and its K103N mutant. *Bioorg. Med. Chem. Lett* 2006;16:2748–2752. [PubMed: 16503141]
 59. Campiani G, Ramunno A, Maga G, Nacci V, Fattorusso C, Catalanotti B, Morelli E, Novellino E. Non-nucleoside HIV-1 reverse transcriptase (RT) inhibitors: Past, present, and future perspectives. *Curr. Pharm. Design* 2002;8:615–657.
 60. Rodríguez-Barrios F, Balzarini J, Gago F. The molecular basis of resilience to the effect of the Lys103Asn mutation in non-Nucleoside HIV-1 reverse transcriptase inhibitors studied by targeted Molecular Dynamics simulations. *J. Am. Chem. Soc* 2005;127:7570–7578. [PubMed: 15898808]
 61. Barreiro G, Kim JT, Guimarães CRW, Bailey CM, Domaol RA, Wang L, Anderson KS, Jorgensen WL. From docking false-positive to active anti-HIV agent. *J. Med. Chem* 2007;50:0000–0000. In press

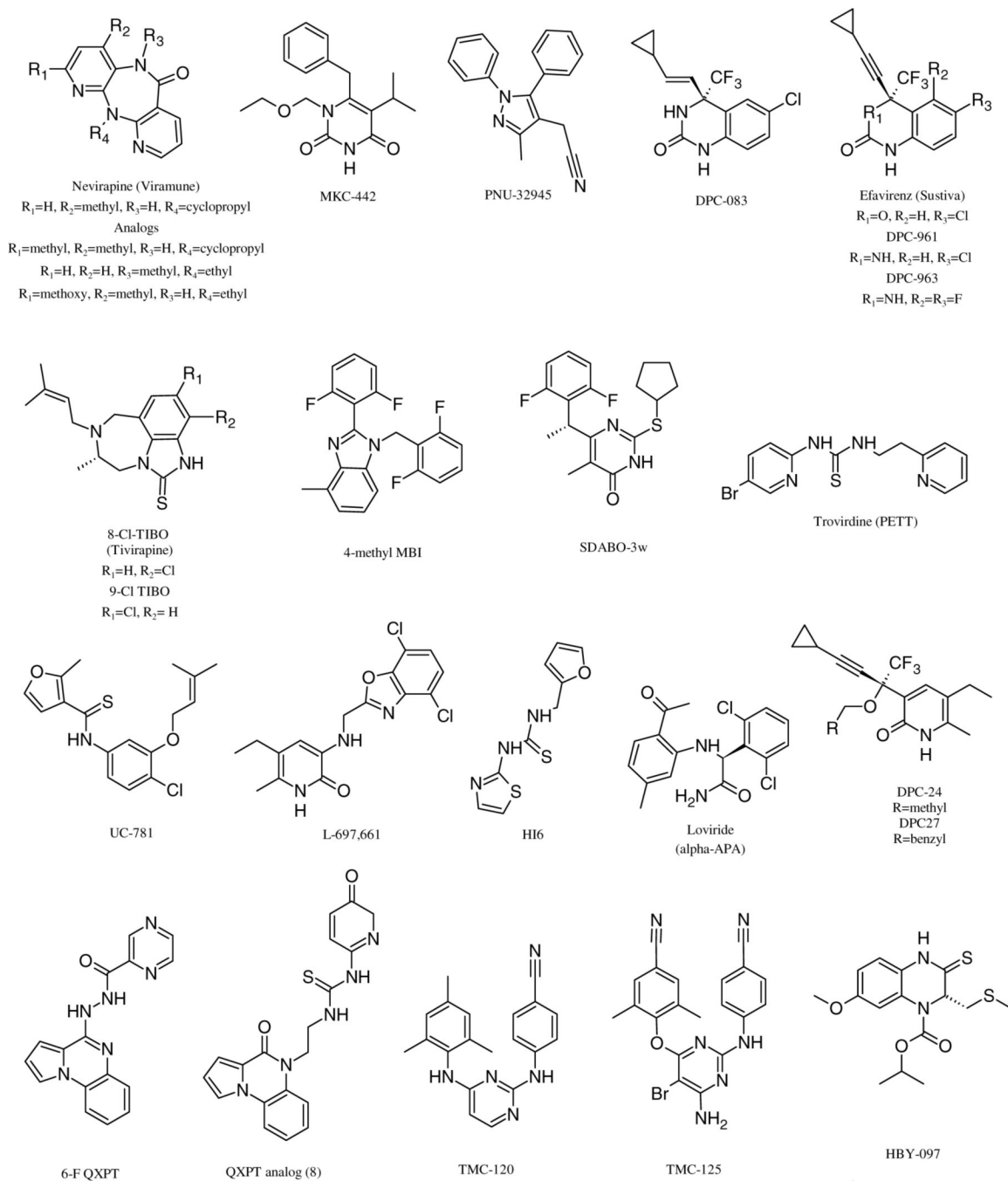


Figure 1.
 The 26 known non-nucleoside HIV-RT inhibitors used in the virtual screening.

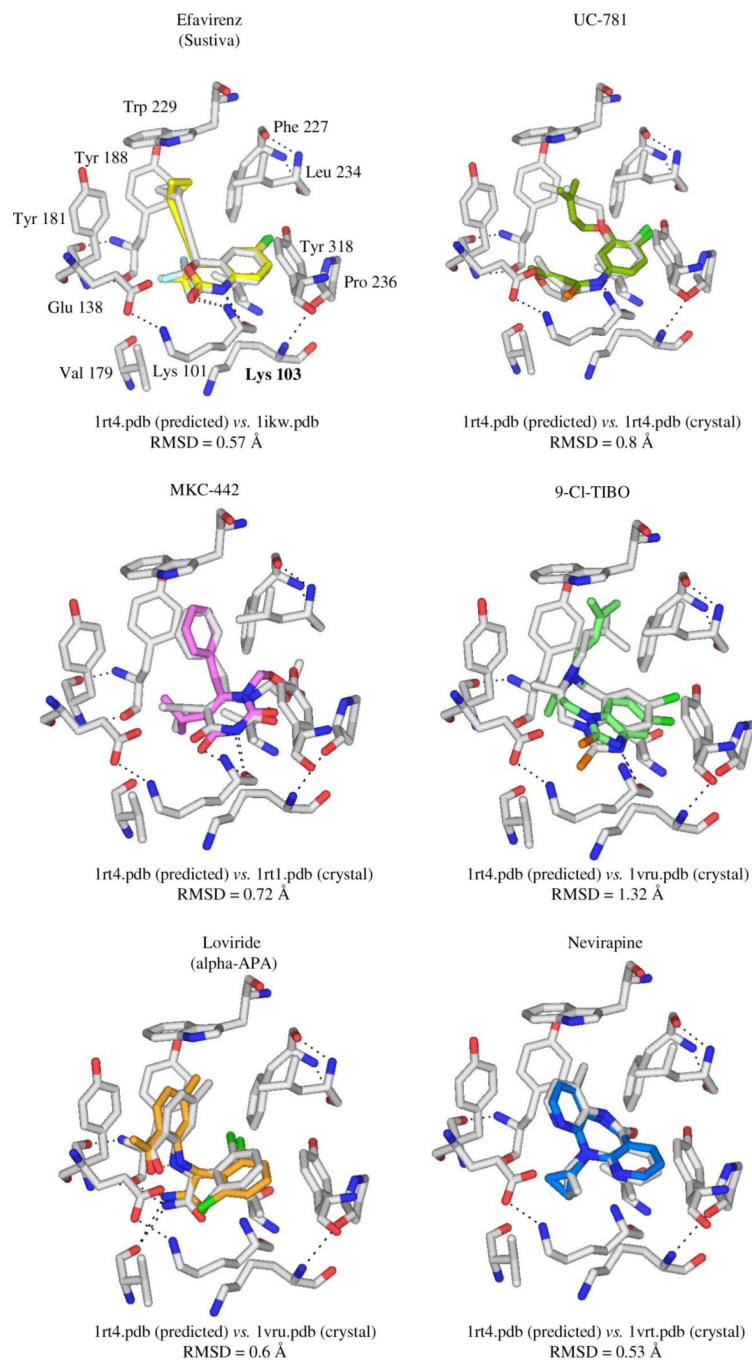


Figure 2. Comparison between the docked (light gray) and the observed crystal structures for six NNRTIs. The RMSd values are noted. All NNRTIs were docked into the 1rt4 structure.

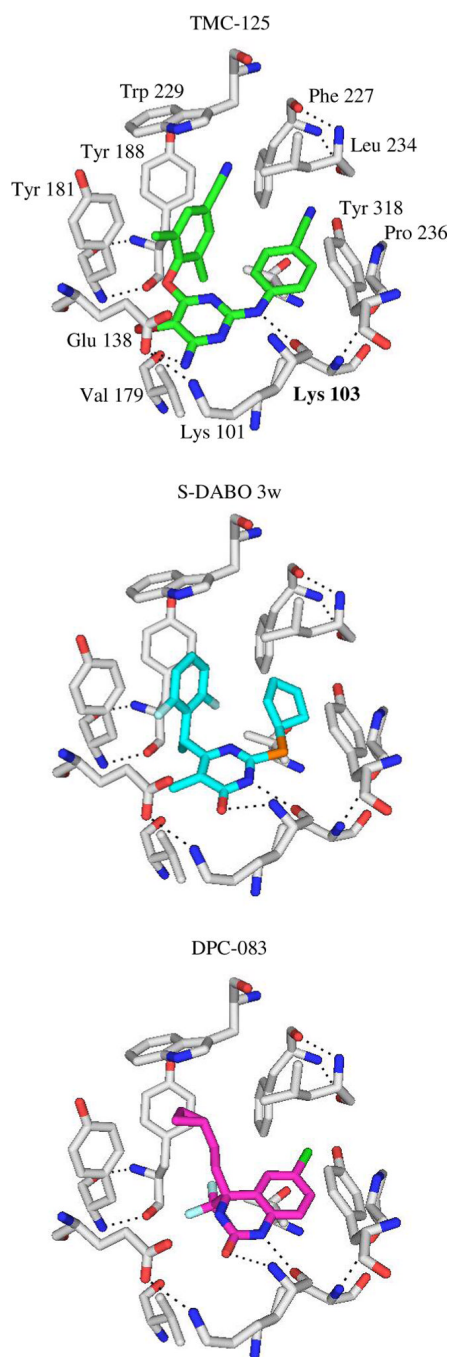


Figure 3. Docking poses for three additional known NNRTIs, TMC-125, S-DABO-3w, and DPC-083.

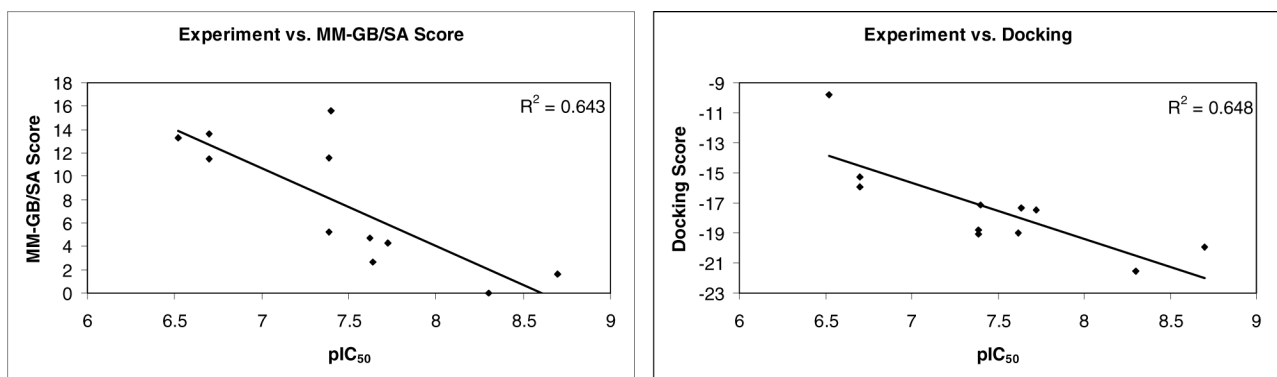


Figure 4. MM-GB/SA Score (left) and Glide XP function (right) versus pIC₅₀ for 11 NNRTIs.

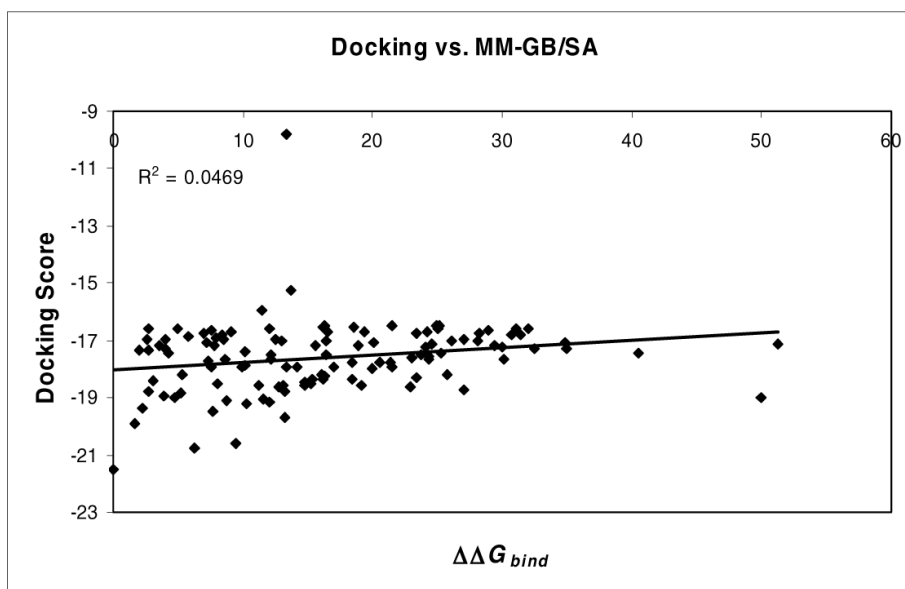


Figure 5. $\Delta\Delta G_{bind}$ versus XP docking score. S-DABO-3w, the ligand with the most favorable binding energy (ΔG_{bind}), was used as reference to obtain $\Delta\Delta G_{bind}$.

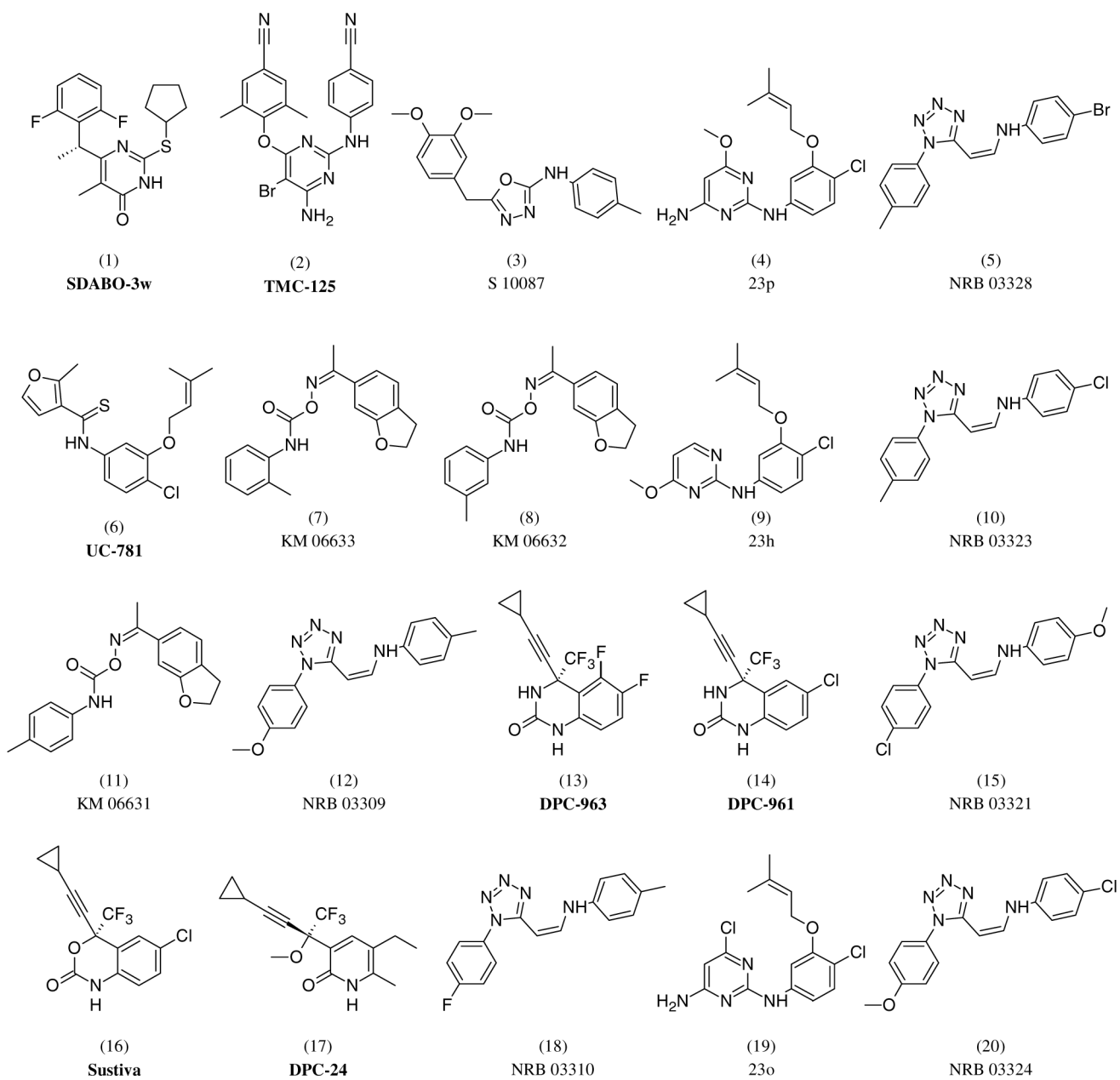


Figure 6.
Top 20 compounds from the MM-GB/SA post-scoring after docking into wild-type HIV-RT.

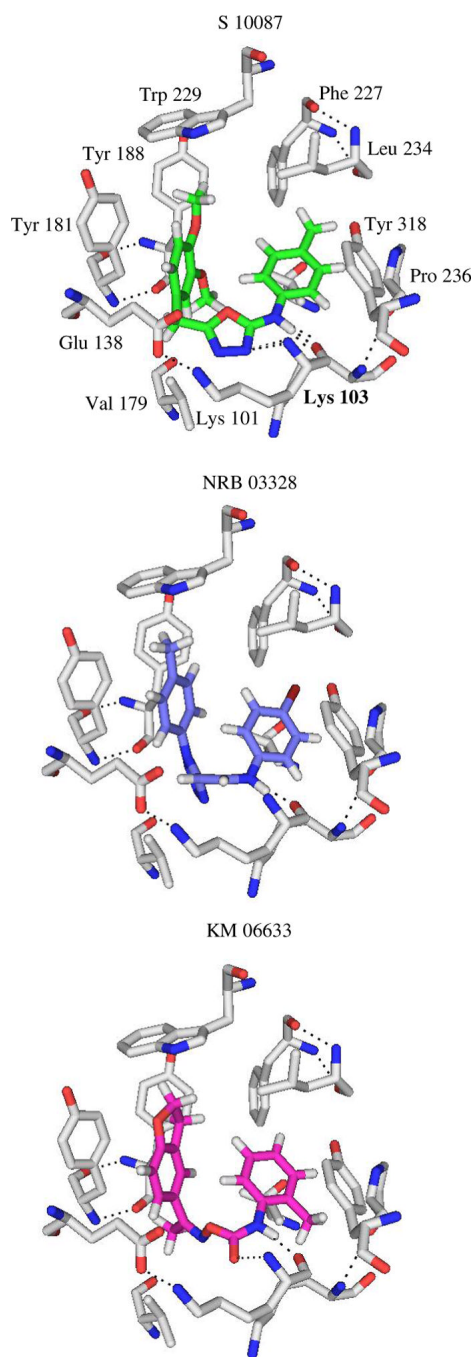


Figure 7.
Energy-minimized complexes between HIV-RT and S10087, NRB03328, and KM06633.

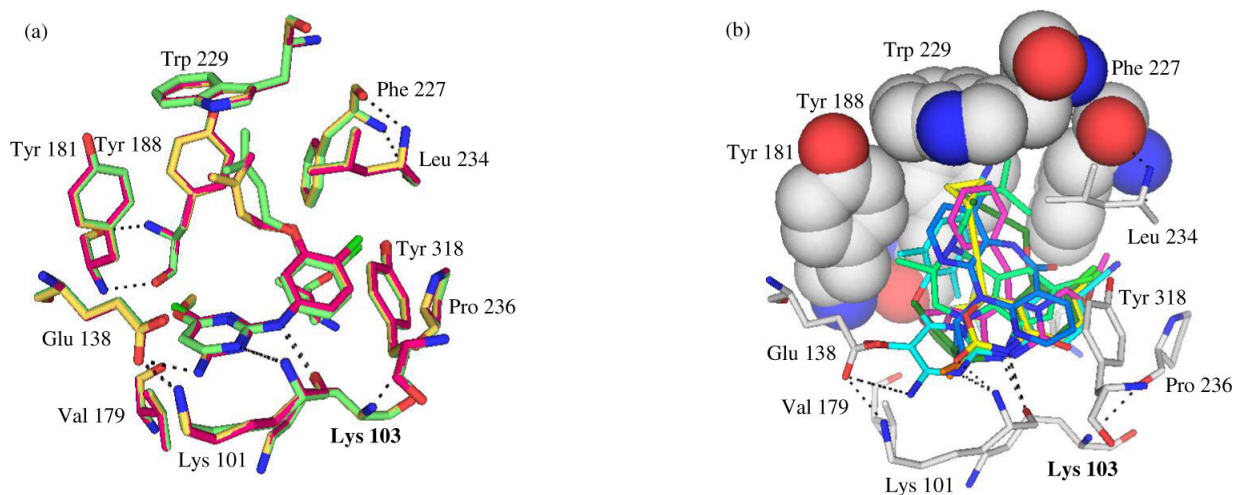


Figure 8.

(a) Overlay of the energy-minimized complexes for the best scoring 2-pyrimidines (23p (yellow), 23h (green), and 23o (magenta)). (b) Hydrophobic interactions between the arene pocket (CPK) and unsaturated groups; 3,3-dimethylallyloxy in UC-781 (dark green), methylpyridinyl in nevirapine (blue), benzyl in MKC-442 (magenta), 3,3-dimethylallyl in 9-Cl TIBO (light green), ethynylcyclopropyl in Sustiva (yellow), and phenoxy in TMC-125 (light blue).

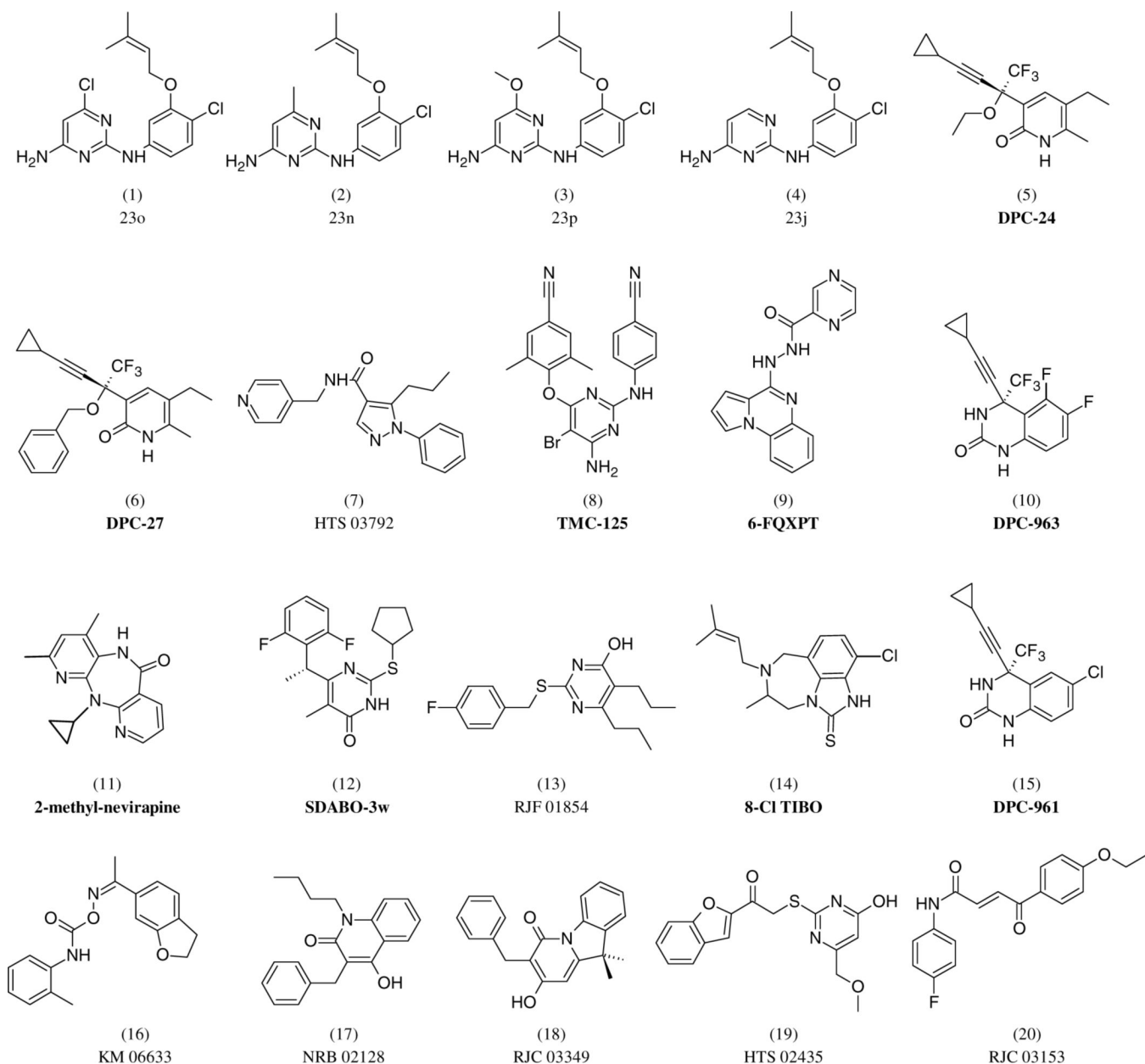


Figure 9. Top 20 compounds ranked by the MM-GB/SA post-scoring after docking into the K103N variant of HIV-RT.

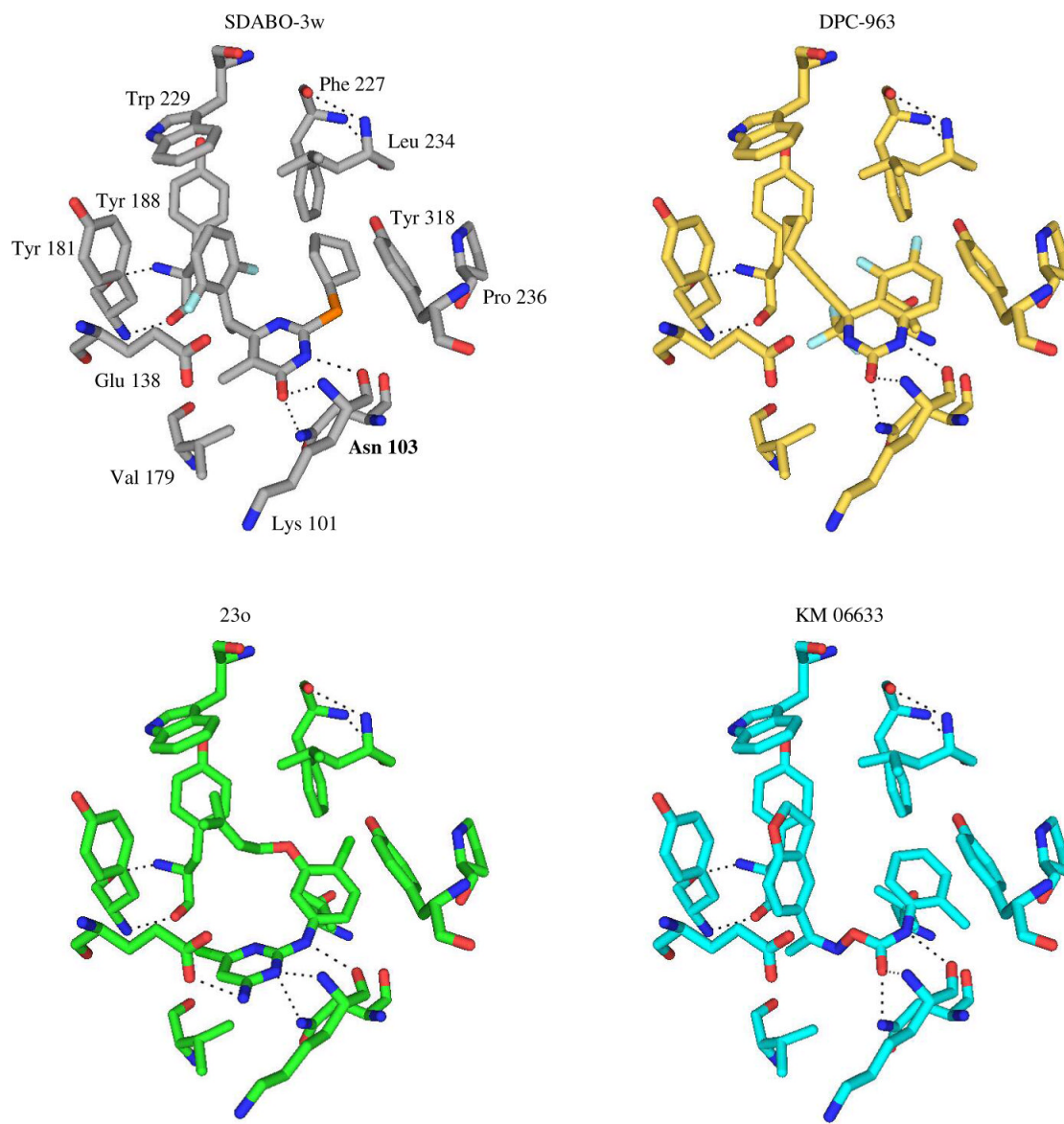


Figure 10. Energy-minimized complexes between K103N-RT and S-DABO-3w, DPC-963, 23o, and KM06633. All four ranked among the best 20 compounds for both HIV-RT and K103N-RT.

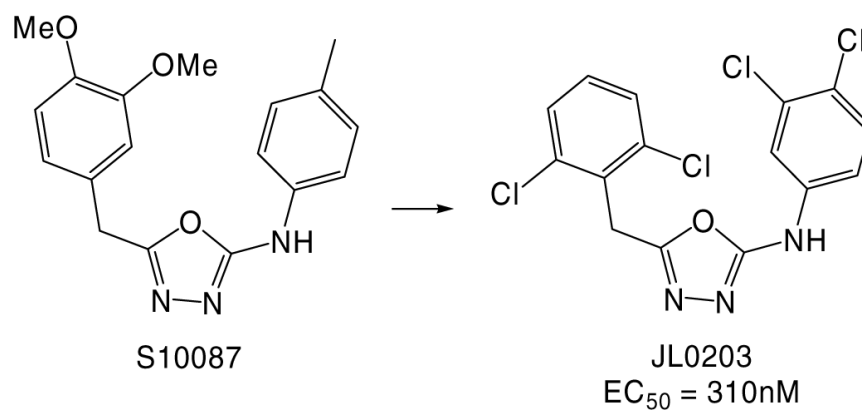


Figure 11. Modifications of S10087 that generated the anti-HIV agent JL0203.

Table 1

MM-GB/SA results for wild-type HIV-RT.^a

Compounds	$\Delta\Delta G_{bind}$	$T\Delta S_{conf}$	ΔE_{solv}	ΔE_{intra}	E_{VDW}	E_{Elect}	E_{PTN}
S-DABO-3w	0.0	0.5	3.6	0.8	-46.4	-17.9	-947.3
TMC-125	1.6	0.5	8.4	5.5	-55.2	-19.6	-944.6
S10087	2.0	1.4	8.2	3.7	-45.8	-20.4	-951.7
23p	2.3	1.9	7.3	2.3	-48.0	-21.2	-946.5
NRB03328	2.6	0.1	7.1	4.2	-46.6	-14.2	-954.6
UC-781	2.7	2.1	4.4	5.4	-51.7	-14.6	-949.5
KM06633	2.7	1.3	5.9	1.0	-46.0	-13.9	-952.1
KM06632	2.7	1.9	4.6	0.8	-46.4	-13.3	-951.4
23h	3.0	2.1	6.0	1.6	-47.1	-17.6	-948.6
NRB03323	3.5	0.0	4.9	4.6	-45.4	-14.2	-953.1
KM06631	3.9	1.2	7.3	2.4	-46.2	-14.5	-953.0
NRB03309	4.0	0.8	7.6	3.4	-45.2	-14.5	-954.6
DPC-963	4.3	0.0	4.5	1.0	-34.5	-19.9	-953.5
DPC-961	4.7	0.0	5.0	0.9	-37.5	-16.8	-953.5
NRB03321	4.9	1.0	8.0	3.7	-47.5	-13.1	-953.9
Efavirenz	5.2	0.0	2.4	0.9	-38.2	-13.6	-952.8
DPC-24	5.3	1.7	2.1	5.6	-46.2	-13.4	-951.1
NRB03310	5.8	0.4	5.5	3.5	-43.6	-11.3	-955.3
23o	6.3	1.8	6.9	3.6	-45.8	-20.6	-946.3
NRB03324	6.9	0.8	7.7	3.4	-45.1	-14.5	-952.0

^aThe known NNRTIs are in bold. $\Delta\Delta G_{bind}$ was obtained by calculating relative binding energies using S-DABO-3w, the ligand with the most favorable binding energy, as reference. E_{PTN} is the protein energy, E_{VDW} and E_{Elect} are the van der Waals and electrostatic interaction energies, ΔS_{conf} , ΔE_{intra} and ΔE_{solv} are the conformational entropy, intramolecular, and desolvation penalties for each ligand upon binding (see eq 4).